Supporting Information

Barquilla et al. 10.1073/pnas.1210465109

SI Materials and Methods

Trypanosome Strains, DNA Plasmid Constructs, and RNAi. Monomorphic bloodstream *Trypanosoma brucei brucei* 1.2 (clone 221a derived from Lister 427) (1) was cultured in Hirumi's modified Iscove's medium (HMI-9) supplemented with 10% heat-inactivated FBS at 37 °C and 5% CO_2 (2). Procyclic forms of the monomorphic trypanosome strain 1313-514 (3) and the pleomorphic strain AnTAT 1.1 (4) were cultured in SDM-79 medium supplemented with 10% FBS at 28 °C and room air (5). In vitro differentiation of bloodstream-to-procyclic forms was performed using modified Differentiating Trypanosome Medium (DTM) supplemented with 15% FBS (6). Slender and stumpy forms of pleomorphic AnTAT 1.1 were obtained from BALB/c mice 3 and 6 d postinfection, respectively. Blood was collected in heparin-containing tubes and centrifuged at 1,000 × *g* for 6 min at room temperature. Then cells were washed twice with separation buffer (SB) (44 mM NaCl, 57 mM Na_2HPO_4, 3 mM NaH_2PO_4) supplemented with 10 mM glucose. The buffy coat was resuspended in SB-glucose and passed through a diethylaminoethylcellulose DE52 (Whatman) anion exchange chromatographic column, and trypanosomes were collected in the flow-through fraction. Cells were maintained at 37 °C during the process.

The GeneDB database accession number for the *T. brucei* target of rapamycin 4 (TbTOR4) gene is Tb927.1.1930. DNA fragments corresponding to both the 5′ and 3′ regions of the TbTOR4 ORF were amplified by PCR using the primers: 5′ ORF TbTOR4: F-GGGGGATCCGAGTCCGTGCTACAACAA; R-CCCCTCGAGTCACACGTAACCATCAATATC; 3′ ORF TbTOR4: F-GGGGGATCCAGTTGGGGGTTAATGACC; and R-CCCCTCGAGTCACGGTTCCATCGCCTTCTG. The PCR product was cloned in the p2T7bla plasmid, widely used for tetracycline-inducible expression of target dsRNA in *T. brucei*. In addition, the 5′ TbTOR4 PCR product was cloned into 5′pET-28a (Novagen) and transformed into *Escherichia coli* BL21 and *E. coli* KRX, respectively.

The TbLST8 (Tb10.61.0700) ORF was PCR amplified (primers: Full ORF TbLTS8, F-CCCGGCCGGCCCTTAAGATGAGCTCTACATTTATTATA and R-GGGGGATCCCTATTGGTTTTTCTTCCTTTC) and was cloned into pTAP1N (7) plasmid. An amino-terminal tandem affinity purification (TAP)-tagged version of TbTOR4 was generated using the primers describe above and was inserted into a pTAP1N plasmid. TAP-*T. brucei* major vault protein (TbMVP) and recombinant protein were generated by amplifying the TbMVP (Tb927.5.4460) ORF by PCR using the primers 5′-GGCGGATCCATGAGTGATATCATACGAATTAAACGT, 3′-CCGAAGCTTCTCGAGCACGGTGGCGGTGATTACCT. The PCR product was cloned into the pTAP1N vector and 5′pET-28a. The *T. brucei* Armadillo-containing TOR-interacting protein (TbArmtor; Tb927.4.2470) ORF was amplified and cloned into 5′pET-28a plasmid using the primers 5′-CGGGATCCATGGAGCTACTCAACGTGTTAC and 3′-CCCCAAGCTTCTCGAGTAACTGATCGGAG. Detailed construction information, maps, and DNA sequences of the plasmids are available upon request. myc-Raptor and myc-AVO3 constructs were previously described (8). PCR reactions were performed in a BioRad thermocycler using FastStart Taq DNA polymerase (Roche).

Transfection of DNA constructs into the bloodstream form of a single-marker cell line and selection procedures for the isolation of stable clonal cell lines were performed as described previously (9). To reduce the likelihood of off-target effects, two non-overlapping regions of the TbTOR4 were inserted into the p2T7 (10) RNAi constructs and were evaluated for depletion of the target gene, reduction of cell proliferation, cell-cycle progression, and mild acidic pH resistance. The phenotypes resulting from both RNAi products were similar, with varying penetrance among different clones. At least three clones for each construction were analyzed. The DNA fragment corresponding to the 3′ ORF of TbTOR4 was amplified by PCR from purified genomic DNA.

The limitations of the RNAi technology probably account for the partial depletion of TbTOR4 (55%) compared with the 100% depletion seen in a pure population of stumpy pleomorphic trypanosomes in the phenotypic analysis.

All attempts to generate a TbTOR4 gain-of-function cell line in the single-marker monomorphic strain have failed. The number of transformant clones expressing the epitope-tagged TbTOR4 was very low and showed TbTOR4 expression levels identical to the parental cell line. Similarly, all attempts to produce a TbTOR4 gain-of-function cell line in a pleomorphic AnTAT 1.1 strain have failed; no transformant clones were obtained, probably because the success rate of AnTAT 1.1 transformation is extremely low.

Animals. The isolation of slender and stumpy forms of the pleomorphic AnTat 1.1 *T. brucei brucei* strain from Balb/C-mice and the generation of rabbit polyclonal antibodies were performed in compliance with policies approved by the Committee on Use and Care of Laboratory Animals of the Instituto de Parasitología y Biomedicina López-Neyra, Consejo Superior de Investigaciones Científicas.

Production of Antibodies. The TbTOR4 protein fragment (amino acids 1562–1885) was expressed and purified as a recombinant protein with a histidine tail to generate the rabbit anti-TOR4 antiserum and the mouse monoclonal antibody. The recombinant fragments used to generate mouse anti-TbArmtor and anti-TbMVP-1 antisera were TbArmtor (Tb927.4.2470) amino acids 1–539 and TbMVP-1 (Tb927.5.4460) amino acids 1–272, respectively. The recombinant proteins were expressed in the KRX *E. coli* strain with a 5′*pET-28a* plasmid induced with 0.1 mM isopropylthio-β-galactoside and 0.1% Rhamnose for 6 h at 37 °C. Soluble recombinant protein was purified with Ni Sepharose 6 Fast Flow (GE Healthcare). Mouse monoclonal anti-TOR4 antibody (5H7) was generated using standard methods. This antibody was tested using TbTOR4-depleted cells by Western blotting and immunofluorescence (IF) assays confirming specificity and lack of cross-reactivity.

Antibody Conditions for Western Blotting Analysis. Rabbit antiserum anti-TbTOR4 (His-TbTOR4) antibody was used at 1:3,000 dilution in PBS with 1-h incubation. 5H7 antibody supernatant was used overnight. We used anti-TbMVP (1:15,000), anti-TbArmtor mouse antisera(1:400), anti-TbPAD1 (1:500) (11), anti-tubulin KMX (1:5,000), and anti-cytosolic marker TbCSM (12).

Multiple Sequence Alignments and Tree Construction. *Trypanosoma brucei* TOR, ATM, ATR, TRRAP, DNA-PK, SMG-1, and LST8 orthologous gene sequences were searched in the National Center for Biotechnology Information public database, and multiple sequence alignments were carried out using Clustal W. Phylogenetic trees generated from alignments (neighbor-joining method) were visualized by using TreeView 32 software. Bootstrap analysis was performed with 1,000 replications. Branch lengths reflect relative distances between distinct PI3K-related kinases (PIKKs).

Gel Filtration. *T. brucei* bloodstream cells (10^9) were harvested by centrifugation, washed in trypanosome dilution buffer(TDB)-glucose, and lysed in buffer A [40 mM Hepes (pH 7.5), 120 mM NaCl, 1 mM EDTA, 10 mM pyrophosphate, 10 mM glycerophosphate, 50 mM NaF, 0.3% CHAPS, and 1× Protease inhibitor cocktail (Sigma)]. Cell extracts were centrifuged at 13,000 × *g* for 15 min at 4 °C, and the supernatants were cleared through a Millipore filter (pore size 0.2 μm). Five milligrams of soluble extract was loaded onto a Superose 6 HR 10/30 column (Amersham). The flow rate was adjusted to 0.5 mL/min, and 1-mL fractions were collected. Elution profiles of TbTOR4 were analyzed by Western blot and compared with the elution profiles of known protein standards (Bio-Rad).

Plating Efficiency. To assess whether TbTOR4 loss of function triggers a unidirectional response in trypanosome, bloodstream forms were transiently depleted of TbTOR1, TbRaptor, and TbTOR4. Reduced expression of these gene products was achieved by adding doxycycline (1 ug/mL) (Sigma) to the medium for 48 h. Then trypanosomes were washed in HMI-9 to remove doxycycline, stop the production of dsRNA, and restore gene expression toward basal levels. Cells were counted, diluted in HMI9 to obtain a final concentration of 20 cells in a total volume of 15 mL, and distributed in 96-well plates (150 μL per well). Plates were incubated at 37 °C with 5% CO_2 for 7–10 d. The reversibility of the process was analyzed by the ability to proliferate upon restoration of protein expression. Proliferation after transient depletion of proteins was scored by counting the number of growth-positive wells. Three independent experiments were performed, and plating was carried out in triplicate. Uninduced and parental cell lines were included as positive controls for proliferation.

TAP and MS Analysis. TAP of LST8 was carried out as described by Rigaut et al. (13) with minor modifications. Expression of TAP-tagged protein in procyclic 1313-514 cells was induced by adding doxycycline to the medium. Then 1.5×10^{10} cells were harvested at a density of 0.8–1.3 × 10^7 cells/mL and were lysed in buffer A with 0.3% CHAPS. Cell extracts were centrifuged at 16,000 × *g* for 20 min at 4 °C. The supernatant was filtered through a Millipore filter (pore size 0.2 μm). We used 150–200 mg of soluble protein for each purification. IgG binding was performed with 100 μL of packed IgG beads for 2 h at 4 °C, with gentle rotation. The IgG beads were washed four times in lysis buffer and twice in TEV-cleavage buffer [10 mM Hepes·KOH (pH 8.0), 120 mM NaCl, 0.5 mM EDTA, 1 mM DTT, 0.3%CHAPS]. TEV cleavage was performed overnight with 100 U of acTEV protease (Invitrogen) at 4 °C with gentle rotation. After proteolytic cleavage of the TAP tag, the supernatants were recovered and used for the second affinity step. One hundred microliters of packed calmodulin beads were added to the recovered supernatant in a total volume of 1,200 mL, in calmodulin binding buffer [10 mM Hepes·KOH (pH 8.0), 120 mM NaCl, 1 mM $MgCl_2$, 1 mM imidazole, 1 mM CaCl2, 0.3%CHAPS]. Calmodulin binding took place for 4 h at 4 °C, with gentle rotation. After binding, the beads were washed four times in calmodulin washing buffer [50 mM ammonium bicarbonate (pH 8.0), 75 mM NaCl, 1 mM MgOAc, 1 mM CaCl2) and eluted with 2× Laemmli protein-loading buffer (4% SDS, 20% glycerol, 0.2 M DTT, 0.004% bromophenol blue, and 0.125 M Tris·HCl).

Protein samples were analyzed in SDS/PAGE gel (20–6% gradient resolving gel with 4% stacking gel) at 150 V. LST8-TAP coprecipitated material was separated by SDS/PAGE, and Coomassie Brilliant Blue G250-stained bands present in the TAP-LST8 lane were excised for identification.

TAP purification of TbTOR4 and TbMVP was carried out using 1.4×10^{11} procyclic *T. brucei* cells harvested, washed, and supplemented with Protease Inhibitor Mixture (Roche) and 1 mM PMSF. Cell pellets were lysed in 50 mL of lysis buffer B [40 mM Hepes (pH 7.5), 120 mM NaCl, 1 mM $CaCl_2$, 10 mM pyrophosphate, 10 mM glycerophosphate, 10 mM NaF, 0.3% CHAPS, and 1× protease inhibitor cocktail (Roche)]. Lysis and tandem affinity purification were carried as for TAP-LST8.

TAP-TbTOR4 and TAP-MVP coprecipitated material was run on SDS/PAGE gels. Electrophoresis was stopped when the front dye barely passed into the resolving gel, ensuring concentration of all proteins into a unique band. Staining was performed using SYPRO Ruby protein gel stain (Sigma).

Protein Identification by Liquid Chromatography Coupled to MS/MS. Gel slices were digested with trypsin. After reduction with DTT (10 mM) and alkylation of Cys groups with iodoacetamide (50 mM), modified porcine trypsin (Promega) was added at a final trypsin: protein ratio of 1:50. Digestion proceeded overnight at 37 °C. After digestion, samples were vacuum dried and were dissolved in 1% acetic acid for analysis by liquid chromatography-MS.

The resulting tryptic peptide mixtures were subjected to nano-liquid chromatography coupled to MS for protein identification. Peptides were injected onto a C-18 reversed-phase (RP) nano-column (100 mm i.d., 12 cm) (Mediterranean Sea, Teknokroma) and were analyzed in a continuous acetonitrile gradient consisting of 0–43% B (95% acetonitrile, 0.5% acetic acid) over 90 min and 50–90% B over 1 min. A flow rate of *ca*. 300 nL/min was used to elute peptides from the RP nano-column to an emitter nanospray needle for real-time ionization and peptide fragmentation on an LTQ-Orbitrap mass spectrometer (Thermo Fisher). An enhanced Fourier transform (FT)-resolution spectrum (resolution = 60,000) followed by the MS/MS spectra from the five most intense parent ions were analyzed along the chromatographic run (130 min). Dynamic exclusion was set at 0.5 min.

MS/MS spectra were extracted, and the charge state was deconvoluted by Proteome Discoverer 1.0 build 43 (Thermo Fisher Scientific) for protein identification. All MS/MS samples were analyzed using SEQUEST version 1.0.43.2 (Thermo Fisher Scientific). Sequest was set up to search Trypanosoma. fasta (1.0, 30,582 entries). Searching was performed assuming full trypsin digestion. Two mixed cleavages were allowed, and an error of 15 ppm or 0.8 Da was set for full MS and MS/MS spectra searches, respectively. All identifications were performed by a Decoy database search; false discovery rate analysis was set at 0.05 by applying the corresponding filter (Score versus Charge state). Oxidation in M was selected as dynamic modification. Scaffold version Scaffold_3_00_08 (Proteome Software Inc.) was used to validate MS/MS-based peptide and protein identifications.

Coimmunoprecipitation. TbRaptor and TbAvo3 coimmunoprecipitations were carried out using 10^9 cells washed and lysed in 1 mL of lysis buffer A. Total cell extracts were centrifuged at 13,000 × *g* for 15 min at 4°. The soluble fraction was precleared with 40 μL Sepharose 4B (Sigma) for 2 h at 4 °C. Twenty microliters of μL protein G-Sepharose were incubated with the indicated antibodies for 1 h, washed twice, and then added to the cleared cell extract. The suspension was rotated for 4 h at 4 °C and washed four times with lysis buffer. Coimmunoprecipitated material was resolved in a 6–8% SDS/PAGE, transferred to nitrocellulose membranes, and analyzed by Western blotting using specific antibodies described previously (8).

TbArmtor and TbTOR4 coimmunoprecipitation experiments used 2.5 10^9 cells lysed in 1 mL of lysis buffer B (described above). Total cell extracts were centrifuged at 13,000 × *g* for 15 min, and soluble fractions were cleared with 40 μL of Sepharose 4B (Sigma-Aldrich) for 1 h. After clearing, 15 μL of the mouse anti-TbArmtor and rabbit anti-TbTOR4 sera or unspecific antibody were added to supernatants and incubated for 2 h at 4°. Protein G-Sepharose (40 μL, 50% slurry) (Sigma-Aldrich) was added to each sample and rotated for 1 h. Immunoprecipitates

were washed five times with lysis buffer. Finally, beads were resuspended in 2× Laemmli sample buffer, resolved in a 6–8% SDS/PAGE, and transferred to nitrocellulose membranes. The coimmunoprecipitated material was detected by Western blotting analysis using specific antibodies.

Quantitative RT-PCR. Total RNA was extracted from 5×10^7 bloodstream-form trypanosomes using the High Pure RNA Isolation Kit (Roche) according to the manufacturer's recommendations. The amount of total RNA was quantified by spectrophotometric assay using the NanoDrop system. cDNA was made using 2 μg RNA and 300 nmol random primers in a 25-μL volume with 100 units of SuperScript III First-Strand Synthesis System (Invitrogen) for 30 min at 50 °C. Quantitative PCR assays were performed in an iCycler IQ real-time PCR detection system (Bio-Rad Laboratories); 20-μL reactions were set up containing 1 μL cDNA, 0.5 μmol of specific reverse and forward primers, 7 μL of double-distilled water, and 10 μL of PerfeCtaTM SYBR Green SuperMix for iQ (Quanta Biosciences). The primer sequences were

ESAG11: 5′-ACAAACAAGGCTCTGCAGGT, 3′-TCCTTCACCAAACAACACCA
Histone H4: 5′-GCGAAGGGTAAGAAGAGTGG, 3′-CACGCACCTCGTCGTAGATA
TAO: 5′-TGGGGACACACTCAACTGAA, 3′-GTGTATCAACGAGGCCGTTT
Control (Tb10.389.0540): 5′-TTGTGACGACGAGAGCAAAC, 3′-GAAGTGGTTGAACGCCAAAT
PAD1: 5′-TCATGGTTTCGCCATTCTCGTAACC, 3′-CTCAGCCACTTCTCTCCTACAACAC
VSG221: 5′-AGCTAGACGACCAACCGAAGG, 3′-CGCTGGTGCCGCTCTCCTTTG
Procyclin: 5′-ATGGCACCTCGTTCCCTTTA, 3′-GAATGCGGCAACGAGACCAA
MYO: 5′-CTGCAGAACAAGCACGGCATTT, 3′-ACGCTCAACAGTGGCAGTGAAA
Tubulin: 5′-AGGCAACGGGAGGTCGCTATG, 3′-GGGATGGGATGATGGAGAAAG
PAD2: 5′-AGGGTGATGCCAAAGAACAC, 3′-TACCCACACCGTTGAGAACA

Amplification was carried out at for 2 min 95 °C, followed by 35 cycles of 95 °C (30 s), 60 °C (30 s), and 72 °C (1 min). A melting curve analysis was performed from 55–95 °C with an acquisition every 10 s to test primer dimer formation. No-RT and no-template controls were run in each experiment. Three independent clones were studied, each in triplicate. The gene expression level was measured using the comparative cycle threshold (Ct) method. cDNA obtained from RNAi-induced cells was compared with cDNA from the original cell line to analyze the relative mRNA expression levels. PI3K was used as the housekeeping gene. All data were analyzed using standard computer software. Independent samples tests were performed with the Mann–Whitney rank sum test for equality of variance and paired *t* test for equality of means between Ct values of clone subgroups. Significance statistics were determined by *t* test. All P values <0.05 were considered statistically significant.

Fluorescence-Activated Cell Sorting. Cells ($1.5\ 10^6$) were collected by centrifugation at $1,400 \times g$ for 5 min at 4 °C and were washed in TDB-glucose. The cell pellets were suspended gently in 50 μL of TDB and permeabilized by adding 1 μL saponin (25 mg/mL) at room temperature for 3 min. Samples were diluted with TDB to a final volume of 500 μL. RNase and propidium iodide (PI) were added to the suspension to final concentrations of 10 and 20 μg/mL, respectively, and the suspension was incubated at room temperature for 30 min. The fluorescence of PI-stained cells (10,000 cells per sample) was measured with a FACScan flow cytometer using Cellquest software (BD Biosciences). FACS data were analyzed using the cell-cycle distribution platform in FlowJo 8.8.6 software (Tree Star Inc.). Gating was determined with control cells for each experiment, and the same values were used for all experimental conditions. For cell size analysis, the relative size distribution of living trypanosomes was determined by flow cytometry using the forward scatter parameter.

Kinetics of cAMP/AMP Analogs. Nucleotide analogs were obtained from the BIOLOG Life Science Institute and were prepared following the manufacturer's instructions. The treatments with nucleotide analogs were carried out incubating 1.5×10^5 monomorphic cells with 8-pCPT-2′-O-Me-cAMP (10 μM) and Sp-8-pCPT-2′-O-Me-cAMP (10 μM). Cells (10^6) were treated with 8-pCPT-2′-O-Me-5′-AMP (5 μM). Cells were harvested at indicated time points, and whole-cell extracts were lysed in buffer containing 0.3% CHAPS. Cell extracts and loading controls were analyzed by Western blotting using anti-TbTOR4 and anti-TbTOR1 antibodies. Mild acid (pH5.5) resistance analysis to confirm the percentage of stumpy-like forms was performed as described in *Materials and Methods*.

NAD Diaphorase Assay. Cells (10^7) were harvested by centrifugation at $1,400 \times g$ for 10 min at room temperature, washed, and resuspended in TDB. Cell suspensions were air dried in slides for 10 min and fixed in 2.5% glutaraldehyde (Electron Microscopy Sciences) in a humid chamber for 5 min at 4 °C. After extensive washing with PBS, cells were incubated with a phosphate buffer containing NADH disodium salt (2 mg/mL) (Sigma) supplemented with Nitrotetrazolium Blue (0.6 mg/mL) (Sigma) for 2 h in a humid chamber at 37 °C. Then, slides were washed twice in PBS and mounted in ProGold Long antifade reagent (Molecular Probes). Concentrations of NADH and Nitrotetrazolium blue were adjusted empirically by staining stumpy pleomorphic and slender monomorphic trypanosomes as positive and negative controls, respectively. Cells were visualized using a Cell R IX81 Olympus microscope equipped with a 60× oil objective (NA 1.40) (Olympus). One hundred cells per treatment were monitored for the presence of black, dense formazan precipitate to estimate the percentage of diaphorase-positive cells. Two samples for each time point and each experimental condition were analyzed by two independent observers in four independent experiments. Statistical analysis was performed by unpaired *t* test. Slender- and stumpy-enriched samples were processed as negative and positive controls, respectively.

Microscopy. TbTOR4 colocalization analysis was performed by 3D IF and deconvolution as described previously (14). Cells were fixed with 2% paraformaldehyde (PFA) for 20 min and permeabilized with 0.1% Triton X-100 for 20 min. Rabbit polyclonal anti-TbBiP (15) (1:20,000), anti-*Lm*MVAK (16) (1:1,500), and anti-TcPo (17) (1:10,000) antibodies were diluted in 0.5% blocking reagent (Roche) and combined with 5H7. For mitochondrial staining, 10^6 cells were incubated with 10 mM of MitoTracker Red CMXRos (Molecular Probes) for 15 min at 37 °C in TDB-glucose buffer. Cells were washed and fixed in 4% PFA for 20 min at room temperature, and an anti-TbTOR4 IF assay was carried out as described above. Goat anti-mouse Alexa Fluor 488-conjugated and goat anti-rabbit Alexa Fluor 594-conjugated (Invitrogen) were used as secondary antibodies, and cells were stained with DAPI. Stacks (0.2-μm z step) acquisition was performed with a motorized microscope system (Cell R IX81; Olympus) equipped with a 100× NA 1.40 oil objective (Olympus), MT20 illumination system (Olympus), and a charge-coupled device camera (Orca CCD; Hamamatsu Photonics). Deconvolution of 3D images was performed using Huygens Es-

sential software version 2.9 (Scientific Volume Imaging) using an experimentally calculated point-spread function with 0.2-μm TetraSpeck microspheres (Invitrogen). All images displayed in the figures are maximum intensity projections from digitally deconvolved multichannel 3D image datasets. Pseudocoloring and maximum intensity projections were performed using ImageJ software version 1.43 (National Institutes of Health). A colocalization mask (white) was calculated for each nonequalized 8-byte slice and merged with anti-TbTOR4 (green) and the other antibodies (red), with a 50% threshold. IF analysis upon differentiation to the procyclic form was performed using anti-221VSG and anti-procyclin antibodies as described above.

1. Cross GAM (1975) Identification, purification and properties of clone-specific glycoprotein antigens constituting the surface coat of Trypanosoma brucei. *Parasitology* 71:393–417.
2. Hirumi H, Hirumi K (1994) Axenic culture of African trypanosome bloodstream forms. *Parasitol Today* 10:80–84.
3. Biebinger S, Wirtz LE, Lorenz P, Clayton C (1997) Vectors for inducible expression of toxic gene products in bloodstream and procyclic Trypanosoma brucei. *Mol Biochem Parasitol* 85:99–112.
4. Gray AR (1977) Antigenic variation in Trypanosomes with particular reference to Trypanosoma gambiense. *Ann Soc Belg Med Trop* 57:403–408.
5. Brun R, Schönenberger (1979) Cultivation and in vitro cloning or procyclic culture forms of Trypanosoma brucei in a semi-defined medium. Short communication. *Acta Trop* 36:289–292.
6. Vassella E, Roditi I, Braun R (1996) Heterogeneous transcripts of RIME/ingi retroposons in *Trypanosoma brucei* are unspliced. *Mol Biochem Parasitol* 82:131–135.
7. Peñate X, et al. (2009) RNA pol II subunit RPB7 is required for RNA pol I-mediated transcription in Trypanosoma brucei. *EMBO Rep* 10:252–257.
8. Barquilla A, Crespo JL, Navarro M (2008) Rapamycin inhibits trypanosome cell growth by preventing TOR complex 2 formation. *Proc Natl Acad Sci USA* 105: 14579–14584.
9. Wirtz E, Leal S, Ochatt C, Cross GA (1999) A tightly regulated inducible expression system for conditional gene knock-outs and dominant-negative genetics in Trypanosoma brucei. *Mol Biochem Parasitol* 99:89–101.
10. Wang Z, Morris JC, Drew ME, Englund PT (2000) Interference of Trypanosoma brucei gene expression by RNA Interference using an integratable vector with opposing T7 promoters. *J Biol Chem*. 275(51):40174–40179.
11. Dean S, Marchetti R, Kirk K, Matthews KR (2009) A surface transporter family conveys the trypanosome differentiation signal. *Nature* 459:213–217.
12. Shahbazian D, et al. (2006) The mTOR/PI3K and MAPK pathways converge on eIF4B to control its phosphorylation and activity. *EMBO J* 25:2781–2791.
13. Chanprasert S, Geddis AE, Barroga C, Fox NE, Kaushansky K (2006) Thrombopoietin (TPO) induces c-myc expression through a PI3K- and MAPK-dependent pathway that is not mediated by Akt, PKCzeta or mTOR in TPO-dependent cell lines and primary megakaryocytes. *Cell Signal* 18:1212–1218.
14. Landeira D, Bart JM, Van Tyne D, Navarro M (2009) Cohesin regulates VSG monoallelic expression in trypanosomes. *J Cell Biol* 186:243–254.
15. Bangs JD, Brouch EM, Ransom DM, Roggy JL (1996) A soluble secretory reporter system in Trypanosoma brucei. Studies on endoplasmic reticulum targeting. *J Biol Chem* 271:18387–18393.
16. Carrero-Lérida J, Pérez-Moreno G, Castillo-Acosta VM, Ruiz-Pérez LM, González-Pacanowska D (2009) Intracellular location of the early steps of the isoprenoid biosynthetic pathway in the trypanosomatids Leishmania major and Trypanosoma brucei. *Int J Parasitol* 39:307–314.
17. Kumar V, Zhang MX, Swank MW, Kunz J, Wu GY (2005) Regulation of dendritic morphogenesis by Ras-PI3K-Akt-mTOR and Ras-MAPK signaling pathways. *J Neurosci* 25:11288–11299.

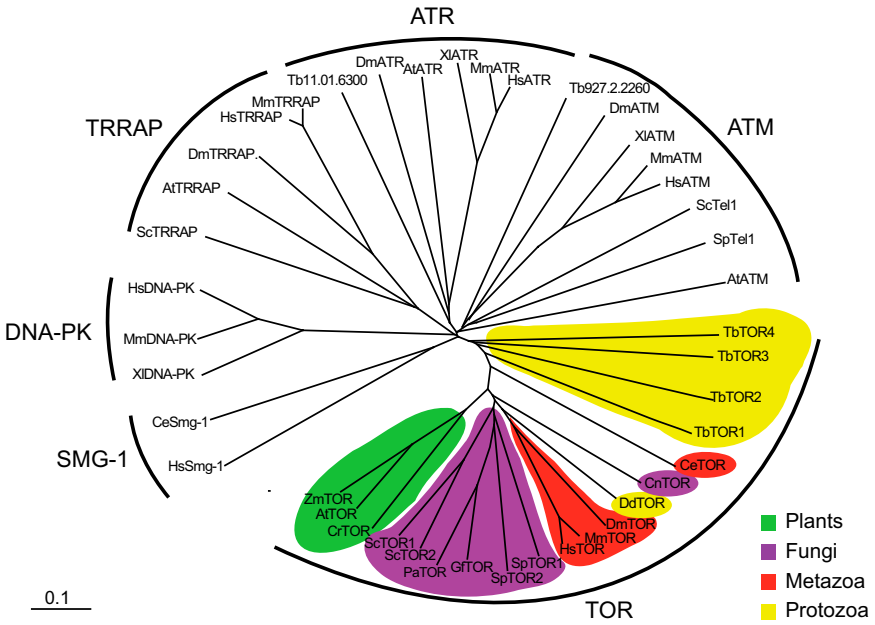

Fig. S1. TbTOR4 belongs to the TOR kinase subgroup within the PIKK superfamily. The neighbor-joining tree was constructed based on amino acid sequences from known and putative PIKKs across Eukarya. The protein sequences used were obtained from the *Trypanosoma brucei* genome (Tb), human (Hs), *Caenorhabditis elegans* (Ce), *Arabidopsis thaliana* (At), *Chlamydomonas reinhardtii* (Cr), *Zea mays* (Zm), *Saccharomyces cerevisiae* (Sc), *Schizosaccharomyces pombe* (Sp), *Podospora anserina* (Pa), *Mus musculus* (s), *Drosophila melanogaster* (Dm), *Cryptococcus neoformans* (Cn), *Dictyostelium discoideum* (Dd), *Xenopus laevis* (Xl), and *Giberella fujikuroi* (Gf). Proteins related to the well-supported TOR, Smg1, DNA-PK, TRAPP, ATR, and ATM clades are grouped in brackets. Highlighted/colored subgroups in the TOR family represent the distribution of the distinct TOR kinases within the Eukarya superkingdom. (The scale bar indicates the number of amino acid substitutions per site.)

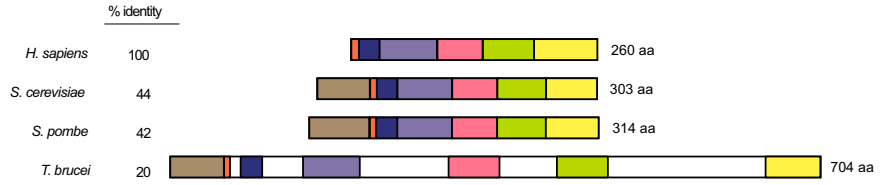

Fig. S2. Schematic representation of the conserved regions shared among LST8 orthologs found in *H. sapiens*, *S. cerevisiae*, *S. pombe*, and *T. brucei*. White boxes represent regions showing no homology in TbLST8. Values indicate the percentage of identity compared with of mammalian LST8.

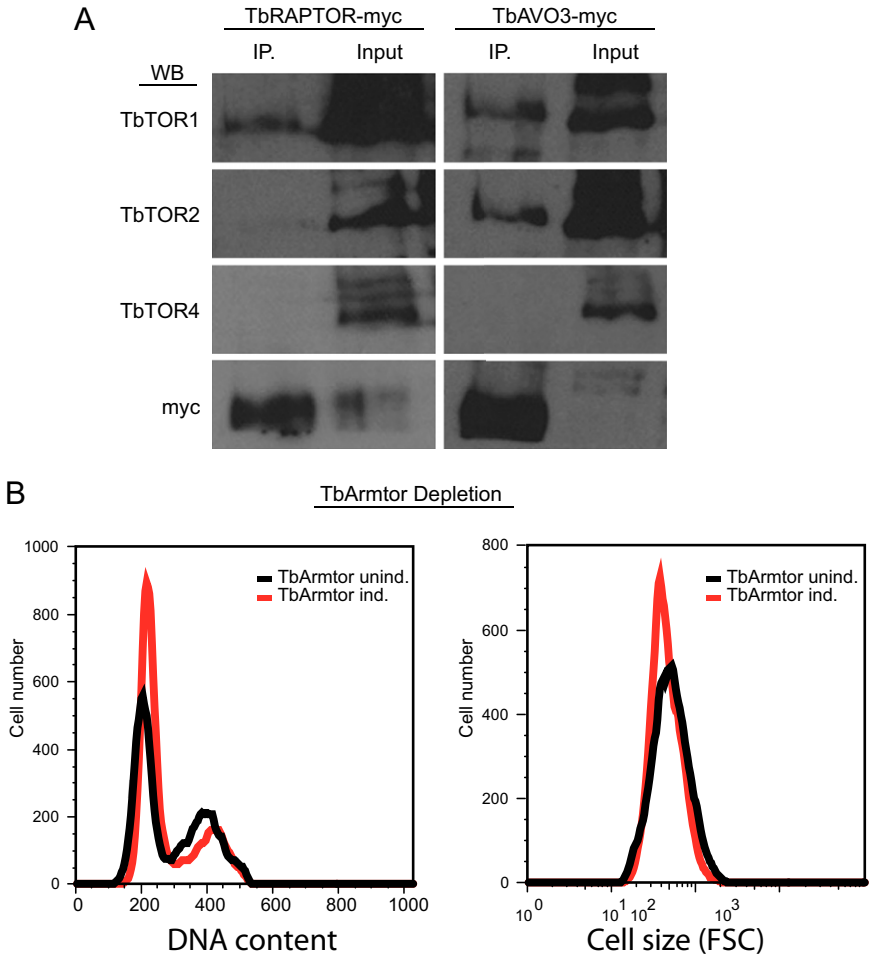

Fig. S3. (*A*) TbTOR4 does not interact with TbRaptor or TbAVO3. Immunoblotting for TbTOR1, TbTOR2, TbTOR4, and myc-tagged proteins was performed on TbRaptor-myc and TbAVO3-myc immunoprecipitates. Whole-cell lysates were prepared from 10^9 bloodstream-form trypanosomes expressing TbRaptor-myc or TbAVO3-myc. Input lanes were loaded with whole-cell lysate corresponding to 5×10^6 cells. TbTOR1 and TbTOR2 were used as a positive controls for interaction with TbRAPTOR and TbAVO3, respectively. (*B*) FACS analysis of DNA content in TbArmtor-depleted cells (TbArmtor ind.) and the uninduced control (TbArmtor unind.) 48 h after RNAi induction with 1 μg/mL doxycycline. FSC, forward scattered light.

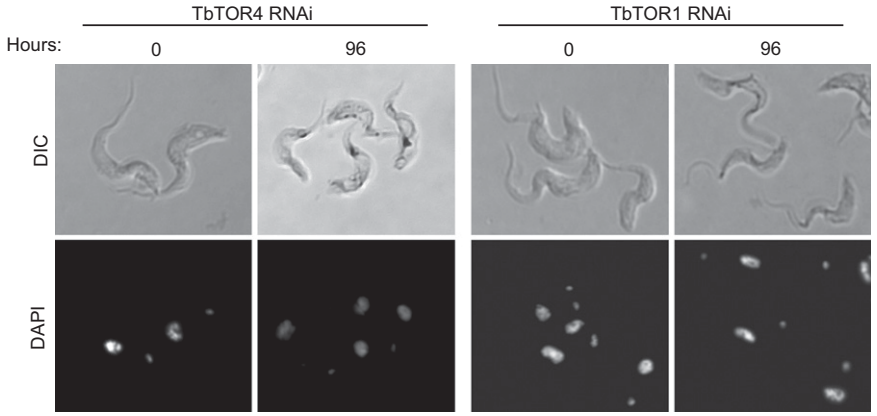

Fig. S4. Diaphorase activity. Fixed trypanosomes were stained with a cytochemical reaction for NADH diaphorase activity and examined with differential interference contrast optics using a 100× oil objective. Formazan precipitates can be seen as dense precipitates staining the mitochondria.

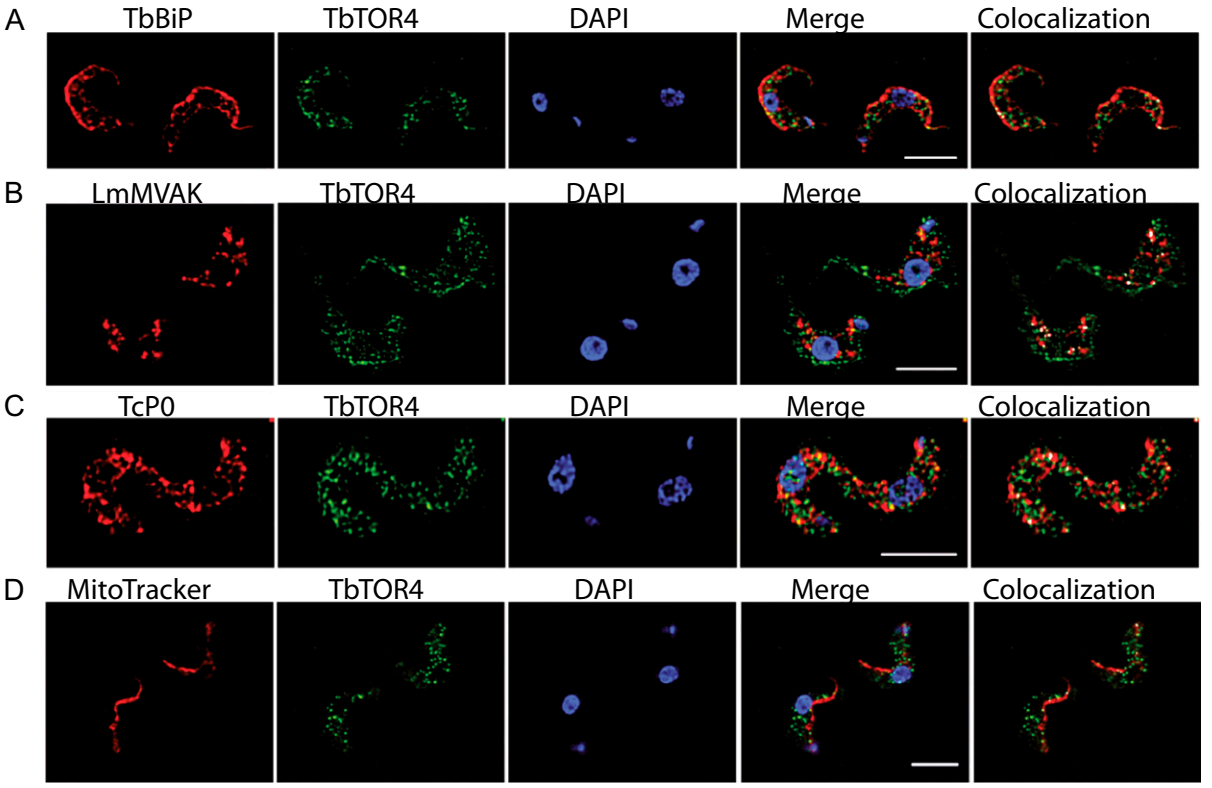

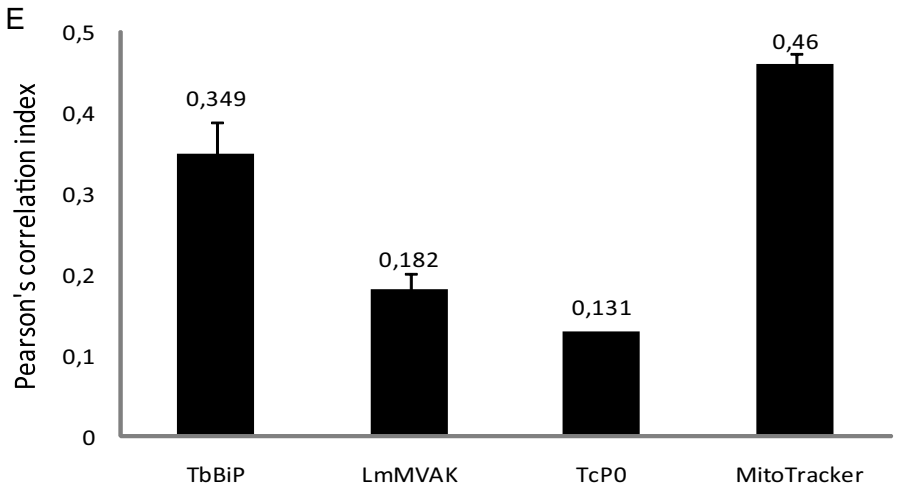

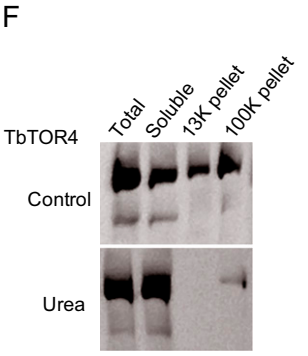

Fig. S5. TbTOR4 colocalization analysis by 3D microscopy. Double indirect IF analysis using anti-TbTOR4 and different cellular markers. TbTOR4 localizes within the cytosol in a punctuated pattern but is excluded from the nucleus and does not colocalize significantly with known organelles. The subcellular localization in bloodstream trypanosomes of TbTOR4 was analyzed using a mouse monoclonal anti-TbTOR4 antibody combined with several rabbit antisera: (*A*) anti-BiP1 (Endoplasmic Reticulum) (1); (*B*) anti-LmMVAK2 (glycosome) (2); (*C*) anti-TcP03 (ribosome) (3) antibodies; and (*D*) MitoTracker as a mitochondrial marker. The antigens were localized by staining with anti-mouse IgG Alexa Fluor 488 (green) and anti-rabbit IgG 594 (red), and the DNA was stained with DAPI (blue). The images are maximum intensity projections of three-channel 3D representative stacks processed by 3D deconvolution. A colocalization mask (white) was calculated for each nonequalized 8-byte slice and merged with anti-TbTOR4 (green) and the other antibodies (red), with a 50% threshold. (Scale bars, 5 μm.) (*E*) Pearson's correlation index (4) calculated from ~10 cells for each antigen, did not show significant colocalization (<0.5) between TbTOR4 and the studied antigens. (*F*) TbTOR4 is partially found in insoluble fractions. The whole-cell extracts were centrifuged sequentially at low (13,000 × *g*) for 30 min) and at high speed (100,000 × *g*) for 2 h to separate the insoluble and the soluble portion. Lysis buffer containing 2M urea was used to release peripheral membrane proteins not anchored in the lipid bilayer.

1. Bangs JD, Uyetake L, Brickman MJ, Balber AE, Boothroyd JC (1993) Molecular cloning and cellular localization of a BiP homologue in Trypanosoma brucei. Divergent ER retention signals in a lower eukaryote. *J Cell Sci* 105:1101–1113.
2. Carrero-Lérida J, Pérez-Moreno G, Castillo-Acosta VM, Ruiz-Pérez LM, González-Pacanowska D (2009) Intracellular location of the early steps of the isoprenoid biosynthetic pathway in the trypanosomatids Leishmania major and Trypanosoma brucei. *Int J Parasitol* 39:307–314.
3. Skeiky YA, et al. (1994) Antigens shared by Leishmania species and Trypanosoma cruzi: Immunological comparison of the acidic ribosomal P0 proteins. *Infect Immun* 62:1643–1651.
4. Bolte S, Cordelières FP (2006) A guided tour into subcellular colocalization analysis in light microscopy. *J Microsc* 224:213–232.

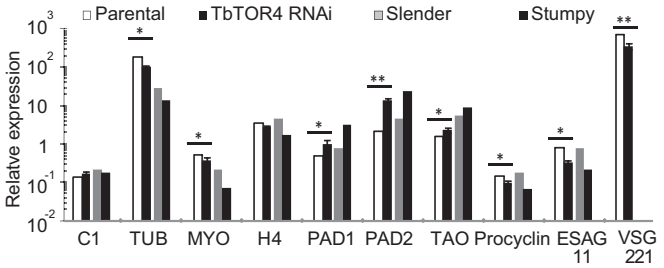

Fig. S6. Graph showing absolute values of the quantitative RT-PCR analysis as an alternative representation of the experimental data in Fig. 3*E*.

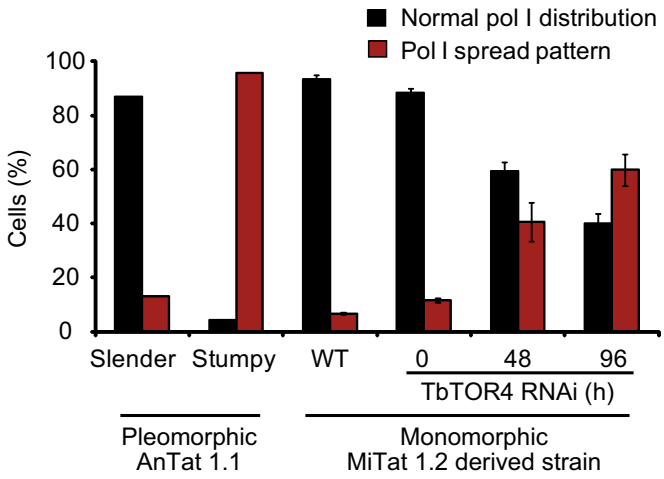

Fig. S7. Statistical analysis of RNA polymerase I (pol I) distribution in pleomorphic cells and TbTOR4-depleted cells. The pattern of RNA polymerase I changes dramatically upon TbTOR4 depletion: RNA polymerase I is delocalized from the normal nucleolar distribution in TbTOR4-depleted cells. More than 50 cells were scored for each condition.

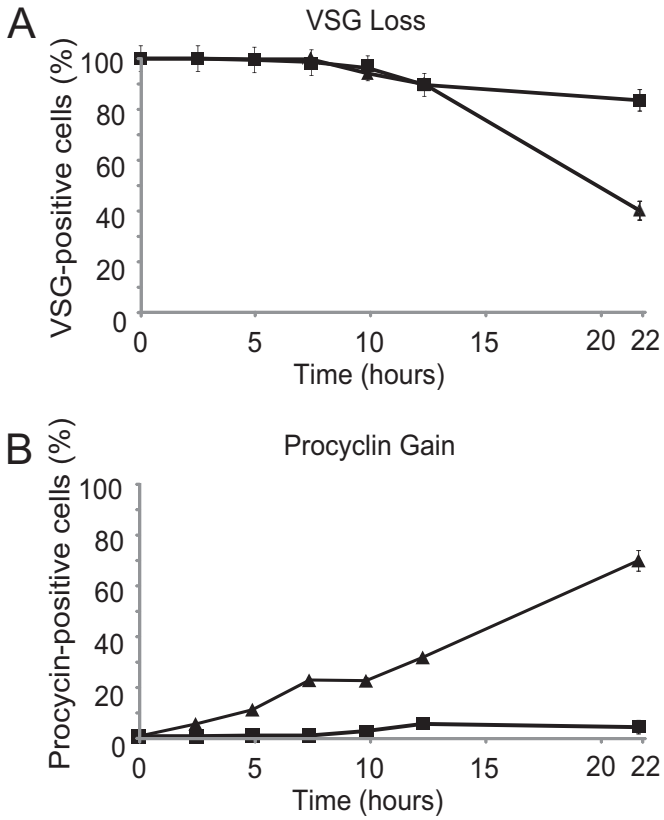

Fig. S8. Bloodstream-to-procyclic form differentiation requires TbTOR1 function. TbTOR1 loss of function impedes bloodstream-to-procyclic differentiation. The in vitro bloodstream-to-procyclic differentiation process was monitored by following changes in expression of the stage-specific markers VSG221 (*A*) and procyclin (*B*). TbTOR1-depleted cells (squares) and the uninduced control (triangles) were exposed to the differentiation signal (DTM medium, 6 mM *cis*-aconitate, 28 °C) at t = 0 h. At the indicated time points, the expression of the procyclin and VSG was followed by indirect IF. Slides were mounted and examined under an Olympus Cell-R microscope.

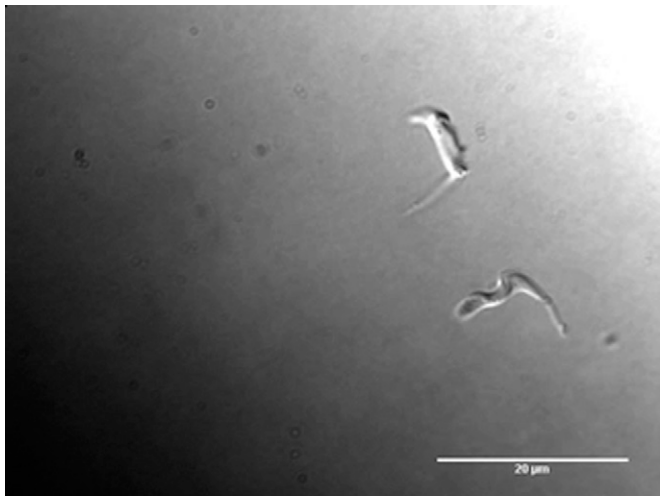

Movie S1. Flagella and cell-motility of wild-type bloodstream trypanosomes (uninduced TbTOR4 RNAi). Time-lapse microscopy movie showing monomorphic bloodstream trypanosomes recorded for 16 s under control conditions. Frames collected using a 100× objective are displayed at a rate of 25 frames/s.

Movie S1

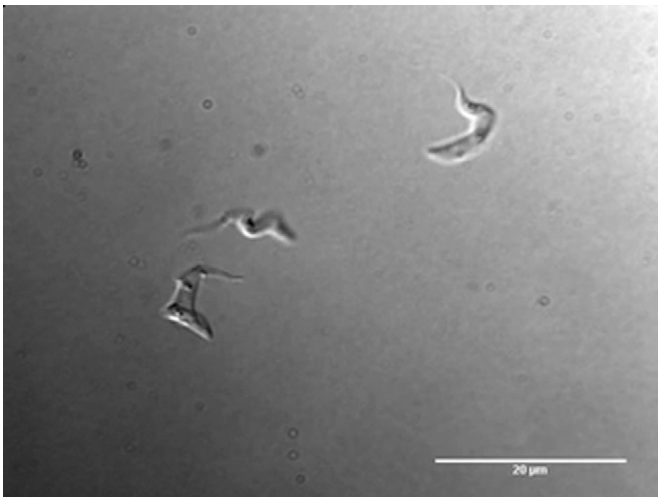

Movie S2. Stumpy-like motility of TbTOR4-depleted trypanosomes. The motion of the flagella and motility of bloodstream trypanosomes is reduced upon TbTOR4 depletion. Monomorphic bloodstream trypanosomes were recorded for 16 s after 96 h of TbTOR4 depletion. Frames collected using a 100× objective are displayed at a rate of 25 frames/s.

Movie S2